ISSN 1070-3632, Russian Journal of General Chemistry, 2015, Vol. 85, No. 6, pp. 1351–1369. © Pleiades Publishing, Ltd., 2015.
Original Russian Text © S.I. Lopatin, S.M. Shugurov, A.I. Panin, K.A. Emel'yanova, 2015, published in Zhurnal Obshchei Khimii, 2015, Vol. 85, No. 6, pp. 881–900.

Thermochemical Study of Gaseous Salts of Oxygen-Containing Acids: XIX.[1] Tin Salts

S. I. Lopatin, S. M. Shugurov, A. I. Panin, and K. A. Emel'yanova

St. Petersburg State University, Universitetskii pr. 26, St. Petersburg, 198504 Russia
e-mail: sergeylopatin2009@yandex.ru

Received February 9, 2015

Abstract—Reactions of the gas-phase synthesis of tin vanadates, borates, and molybdates were studied. Standard enthalpies of formation and atomization of gaseous salts SnV_2O_6, SnB_2O_4, $Sn_2B_2O_5$, $SnMoO_4$, Sn_2MoO_5, and $SnMo_2O_7$ were determined.

Keywords: high-temperature mass-spectrometry, gas-phase reactions, gaseous tin salts, quantum-chemical calculations

DOI: 10.1134/S1070363215060018

At present seven gaseous salts of tin(II) are known: $SnPO_2$, $SnPO_3$ [2], $SnWO_4$, Sn_2WO_5, SnW_2O_7 [3], $SnMoO_4$, and Sn_2MoO_5 [4]. All these salts were obtained by the gas-phase synthesis *in situ* in a Knudsen camera from corresponding oxides. Gaseous tin(II) oxide, which is thermally stable in a wide temperature range, is a typical cation-forming oxide with base properties. Tin dioxide SnO_2 [5] is most stable in the condensed state. Tin dioxide vapor formation in the temperature range 1250–1540 K mainly follows Eq. (1) and, to a lesser degree, Eq. (2) [5]. A part of tin monooxide (~3%) dimerizes to form Sn_2O_2.

In reducing vaporization conditions, for example during, vaporization of a Sn–SnO_2 mixture [Eq. (3)] [6], vaporization temperature decreases to 1050–1200 K. The vapor phase is presented by Sn_nO_n molecules, *n* value varying from 1 up to 6.

$$SnO_2(s) = SnO(s) + 0.5\ O_2(gas), \quad (1)$$

$$SnO_2(s) = 0.5\ Sn_2O_2(gas) + 0.5\ O_2(gas), \quad (2)$$

$$Sn(liq) + SnO_2(s) \rightarrow Sn_nO_n(gas). \quad (3)$$

The oxides V_4O_{10}, B_2O_3, and MoO_3 act as anion-forming species in the high-temperature synthesis of gaseous salts [7–9]. When gaseous oxides V_4O_{10}, B_2O_3, and MoO_3 coexist with gaseous SnO, the corresponding gaseous salts are synthesized [10].

Tin vanadate. Vanadium(V) oxide is a strong oxidizing agent that excluded the use of effusion cells made of molybdenum or tungsten. Molybdenum and tungsten reduce V_2O_5 up to the VO_2 or V_2O_3 oxides [11], which evaporate at much higher temperatures [7], and VO and VO_2 molecules are present in the vapor.

The use of platinum as a cell material is also unacceptable. When V_2O_5 is heated in the absence of a reducing agent, it loses oxygen and can be partially reduced to VO_2 [12], which, in turn, passes in vapor above the platinum melting point (2042 K).

We used an effusion cell made of zirconium dioxide, which is thermally stable up to 2700 K and has no reducing properties.

Peaks of Sn^+, SnO^+, $Sn_2O_2^+$, $V_4O_{10}^+$, and $SnV_2O_6^+$ ions were detected in the mass spectra of vapor above a mixture of SnO_2 and V_2O_5 oxides in the temperature range 1500–1800 K. The ratio of ionic currents depended on the vaporization time and temperature. The intensity of the $V_4O_{10}^+$ ion permanently decreased during the vaporization owing to its higher volatility compared with SnO_2 and also to a partial thermal dissociation giving V_2O_5. When intensities of ionic currents decreased to a background level, the temperature was raised up to 2000 K and peaks of VO_2^+ and $V_2O_4^+$ ions were detected confirming the data of [12].

To determine molecular precursors of the ions in the mass spectrum, we have measured their appearance

[1] For communication XVIII, see [1].

Table 1. Ionization energy (eV) of Sn_2O_2 molecule and tin salts calculated by various quantum-chemical methods

Molecule	Coopmans theorem	$E(M^+)$–E(M) (DFTM06)	Green function method OVGF [27]
Sn_2O_2	8.9	8.6	9.0
SnB_2O_4	11.6	10.8	11.5
$Sn_2B_2O_5$	10.5	9.4	10.4
$SnMoO_4$	11.8	10.6	11.1
Sn_2MoO_5	10.0	9.7	10.0
$SnMo_2O_7$	11.9	10.9	11.4
SnV_2O_6	11.5	10.9	10.9

energies, eV: 15.1±0.5 (Sn^+), 10.6±0.3 (SnO^+), 10±1 ($Sn_2O_2^+$), 10.5±0.3 ($V_4O_{10}^+$), and 11.4±0.5 ($SnV_2O_6^+$). The value of gold ionization energy (9.2 eV) was used as a standard [13]. The appearance energy of SnO^+ is equal to the ionization energy of SnO [13], and the appearance energy of $V_4O_{10}^+$ coincides with the experimental value of V_4O_{10} ionization energy (11.8 eV) [14, 15]. In our experimental conditions the appearance energy of Sn^+ is much higher than the ionization energy of monatomic tin that allows us to state that this ion is a product of dissociative SnO ionization. The appearance energy of $Sn_2O_2^+$ coincides with the ionization energy of Sn_2O_2 (9.8±0.5 eV) [6] within the limits of experimental error. Comparison of the appearance energies of $Sn_2O_2^+$ and $SnV_2O_6^+$ with the ionization energies of Sn_2O_2 and SnV_2O_6 molecules calculated by quantum-chemical methods (Table 1) points to their molecular origin.

Partial vapor pressures of molecular species were determined by the method of comparing ionic currents, using gold as the internal pressure standard [16]. In the calculation of partial pressures of molecules we used atomic ionization cross sections [17], the ionization cross section of tin vanadate was multiplied by 0.7 [18]. Enthalpies of reactions involving gaseous tin vanadate were determined by Eqs. (4), (5).

$$\Delta_r H^0\,(0\text{ K}) = T\Delta_r\Phi_T^0 - RT\ln K_e(T), \quad (4)$$

$$\Delta_r H_T^0\,(T) = -R\frac{\partial \ln K_e(T)}{\partial(1/T)}. \quad (5)$$

Here $\Delta_r H^0(0)$, $\Delta_r H^0(T)$, and $\Delta_r\Phi^0(T)$ are the changes in enthalpy and the reduced Gibbs energy of a reaction at the temperatures 0 and T, respectively, R is the gas constant, and K_e is a reaction equilibrium constant.

To find standard enthalpies of gaseous tin vanadate formation, we have determined equilibrium constants of reactions (6) and (7).

$$SnO(gas) + 1/2V_4O_{10}(gas) = SnV_2O_6(gas), \quad (6)$$

$$Sn_2O_2(gas) + V_4O_{10}(gas) = 2SnV_2O_6(gas). \quad (7)$$

Thermodynamic functions of SnO and V_4O_{10} required for the calculation of the reaction enthalpy were taken from the handbook [19], and those of Sn_2O_2 and SnV_2O_6 were calculated by statistical thermodynamics methods in the approximation rigid rotator-harmonic oscillator. The necessary molecular parameters and tin vanadate structure were determined by quantum-chemical calculations. The measured partial vapor pressures of molecular species above the SnO_2-V_2O_5 system and the enthalpies of reactions (6) and (7) at 0 K calculated by equation (4) are presented in Table 2.

The enthalpies of reactions (6) and (7) calculated by Eq. (5) for the center of the experimental temperature range 1526–1745 K (1636 K) are –123±12 and 49±17 kJ, respectively, or, when reduced to 298 K: –129±12 and 51±17 kJ, respectively.

Tin borates. To obtain tin borates by gas-phase synthesis, mixtures of the boron and tin oxides B_2O_3 and SnO_2 were evaporated from a molybdenum effusion cell. In the temperature range 1300–1500 K peaks of $B_2O_3^+$, Sn^+, SnO^+, $Sn_2O_2^+$, $SnB_2O_4^+$, and $SnB_2O_5^+$ ions were detected in the vapor mass spectra. The ratio of ionic currents intensities largely depended on the solid phase composition and temperature.

To determine qualitative and quantitative composition of the vapor, we measured energies of ions appearance in the mass spectrum. The determination of vapor molecular composition was complicated, therefore it should be considered in greater detail. The origin of SnO^+, $Sn_2O_2^+$, and $B_2O_3^+$ ions is connected with direct ionization of the corresponding molecules. The measured appearance energies of these ions (10.6, 10.5, and 14.1 eV, respectively) within the limits of experimental error have coincided with the values of ionization energies of SnO, Sn_2O_2 and B_2O_3 molecules [6, 13]. The appearance energy of Sn^+ ion, 15.2 eV, is considerably greater than the ionization energy of monatomic tin. The presence of Sn^+ ions in a vapor mass spectrum is caused by the dissociative ionization of SnO molecules. The appearance energies of $SnBO_2^+$,

Table 2. Partial vapor pressures of molecular species above the system SnO_2–V_2O_5 and enthalpies of reactions (6) and (7)

T, K	p, atm				$-\Delta_r H^0$(0 K), kJ	
	SnO ($\times10^{-4}$)	Sn_2O_2 ($\times10^{-6}$)	V_4O_{10} ($\times10^{-7}$)	SnV_2O_6 ($\times10^{-6}$)	reaction (6)	reaction (7)
1526	0.25	0.46	0.21	0.62	137.3	–17.0
1526	0.32	0.62	0.14	0.51	134.6	–20.2
1570	0.78	2.37	0.28	1.66	137.3	–17.3
1567	0.64	2.13	0.28	1.19	135.3	–24.6
1568	0.73	2.13	0.21	1.11	134.6	–22.7
1571	0.60	1.90	0.21	1.03	136.3	–23.2
1570	0.52	1.66	0.21	0.87	136.0	–25.8
1570	0.40	1.19	0.21	0.87	139.5	–21.4
1571	0.36	0.95	0.29	0.79	137.9	–24.7
1617	0.85	2.93	0.44	1.63	136.9	–27.3
1617	0.71	1.47	0.44	1.22	135.5	–25.7
1629	0.60	1.07	0.22	1.07	141.5	–16.1
1626	0.53	0.90	2.2	0.90	140.7	–18.3
1630	0.50	8.21	2.2	0.74	139.1	–22.5
1669	0.73	0.23	4.5	1.85	144.7	–22.0
1727	3.77	32.59	1.68	12.44	143.9	–25.0
1725	4.44	9.07	6.28	13.98	133.6	–22.2
1733	3.92	10.51	6.31	13.27	135.2	–26.1
1733	4.33	12.62	5.68	15.61	136.8	–22.5
1739	5.43	13.36	4.86	14.88	134.5	–22.5
1738	5.70	15.46	4.64	23.48	140.6	–10.8
1738	5.70	13.35	4.01	15.65	135.8	–18.3
1739	5.56	11.25	3.38	11.75	133.3	–21.6
1738	4.75	9.84	3.38	10.96	134.5	–21.7
1733	4.60	10.51	3.37	10.14	133.5	–24.7
1741	3.80	8.45	2.96	9.41	136.7	–22.0
1740	4.07	9.15	2.75	9.40	136.2	–22.1
1738	4.88	9.14	2.53	9.39	134.0	–20.9
1738	4.88	7.73	2.11	8.61	134.0	–18.4
1740	4.35	8.44	2.32	9.40	136.4	–18.5
1739	4.21	7.03	2.32	8.61	135.6	–18.4

Table 2. (Contd.)

T, K	p, atm				$-\Delta_r H^0$(0 K), kJ	
	SnO ($\times 10^{-4}$)	Sn_2O_2 ($\times 10^{-6}$)	V_4O_{10} ($\times 10^{-7}$)	SnV_2O_6 ($\times 10^{-6}$)	reaction (6)	reaction (7)
1739	3.80	6.33	2.11	7.83	136.4	–18.2
1740	4.07	6.33	2.11	7.05	133.9	–21.3
1745	3.54	4.94	1.91	5.50	133.4	–23.5
1743	3.67	5.64	1.91	6.83	135.9	–19.1
1738	3.26	4.22	1.69	5.40	134.8	–19.9
1740	3.26	3.52	1.48	5.41	135.9	–15.3
1648	3.53	8.95	0.72	3.99	128.8	–25.6
1646	3.21	18.87	0.54	4.31	133.0	–29.6
1647	3.21	15.90	0.39	3.32	131.7	–30.1
1648	2.89	16.91	0.30	2.88	133.0	–31.2
1655	1.83	11.65	0.30	2.22	136.3	–33.5
1649	1.82	6.63	0.33	1.88	133.0	–31.4
1643	1.07	5.29	0.36	1.66	137.5	–32.8
1648	1.00	3.78	0.48	1.44	134.9	–36.1
1643	0.42	0.89	0.57	1.32	144.2	–20.9
1648	0.36	0.60	0.90	1.10	140.7	–26.9
1649	0.32	0.33	0.90	1.03	141.6	–20.6
1643	0.36	0.43	1.16	1.10	138.6	–25.7
1653	0.30	0.23	1.08	1.13	142.9	–15.8
1653	0.33	0.30	1.35	1.11	139.7	–22.8
1649	0.31	0.23	1.26	1.00	139.3	–21.2
1690	3.77	8.67	2.79	6.52	128.3	–31.5
1567	0.90	–	1.51	2.49	129.6	–
1583	0.87	–	1.19	3.15	135.9	–
1587	1.09	–	1.08	2.10	128.6	–
1594	0.70	–	0.46	1.90	139.5	–
1596	1.03	–	0.34	1.06	128.6	–
1596	0.62	–	0.29	1.46	140.7	–
1668	2.64	–	0.24	1.66	129.7	–
1672	2.07	–	0.24	1.20	128.8	–
1668	0.34	–	0.18	1.06	153.8	–
1690	3.59	–	1.12	3.72	127.6	–
1691	5.38	–	0.56	5.59	132.5	–
1529	0.27	–	0.62	0.46	126.3	–
				Average value	136±5	–23±5

$Sn_2BO_3^+$, $SnB_2O_4^+$, and $SnB_2O_5^+$ ions were not measured owing to low intensities of the ionic currents. To determine the nature of these ions, we were forced to use thermodynamic methods of vapor composition determination, which were connected with a shift in the condensed phase-vapor equilibrium. To determine the vapor composition above the systems $MO–B_2O_3$ (M is an alkaline-earth metal), we used data of [20, 21].

In the mass spectra of vapor above the systems $MO–V_2O_3$ (M = Ca, Sr, Ba) in the temperature range 1400–1500 K peaks of M^+, MO^+, $B_2O_3^+$ and MBO_2^+ ions were detected [20, 21]. The appearance energies of MBO_2^+ ions are, eV: 11.7 ($CaBO_2^+$), 11.2 ($SrBO_2^+$), and 10.7 ($BaBO_2^+$). On standing at a constant temperature and also with increasing temperature break points appeared in the curves of MBO_2^+ ionization effectiveness and the values of appearance energies of ions decreased to 6.2 ($CaBO_2^+$), 5.6 ($SrBO_2^+$), and 5.4 ($BaBO_2^+$) eV. Two noticeably differing values of appearance energies of MBO_2^+ ions and also break points in ionization effectiveness curves point to a dual nature of these ions formation. The higher appearance energies of MBO_2^+ ions correspond to the dissociative ionization of MB_2O_4 molecules [Eq. (8)], and the lower, to the direct ionization of MBO_2 molecules [Eq. (9)].

$$MB_2O_4 + e^- = MBO_2^+ + BO_2 + 2e^-, \quad (8)$$

$$MBO_2 + e^- = MBO_2^+ + 2e^-. \quad (9)$$

The data obtained are confirmed by the calculations for calcium borates [22]. The ionization energies of the CaB_2O_4 and $CaBO_2$ molecules are 10.84 and 6.53 eV, respectively, and the ionization energies of salts of oxygen-containing acids decrease along the calcium-strontium-barium series of cations [13]. In the mass spectra of vapor above the system $MgO–B_2O_3$ peaks of the $MgB_2O_4^+$ ions were detected in addition to the $MgBO_2^+$ ions [23], and above the system $MnO–B_2O_3$, also of the $MnB_2O_4^+$ ions [24].

The above data in combination with our observations has allowed us to make a series of conclusions related to the problem of the interpretation of vapor mass spectra and to the determination of qualitative and quantitative composition of vapor above borate systems.

(1) In the mass spectra of vapor above the $MgO–B_2O_3$, $MnO–B_2O_3$, and $SnO–B_2O_3$ systems peaks of the MBO_2^+ and $MB_2O_4^+$ ions were detected, above the $CaO–B_2O_3$, $SrO–B_2O_3$, and $BaO–B_2O_3$ systems only peaks of MBO_2^+ ions were fixed. At rather low temperatures of the order of magnitude of 1500 K the origin of MBO_2^+ ions is connected with dissociative ionization of MB_2O_4 molecules according to Eq. (8). Molecules MBO_2 appear in vapor at much higher temperatures and in the case of a decrease in the fraction of boron oxide in a system due to selective vaporization.

(2) In the temperature range 1300–1500 K the ratio of intensities of ionic currents of the $SnBO_2^+$ and $SnB_2O_4^+$ ions in the mass spectra of vapor above the $SnO–B_2O_3$ system remains constant within a rather prolonged vaporization, and then increases gradually. The reduction of ionizing voltage (the energy of ionizing electrons) resulted in a decrease in the ratio of intensities of $SnBO_2^+$ and $SnB_2O_4^+$ ionic currents. Substantial growth of the ratio of intensities of $SnBO_2^+$ and $SnB_2O_4^+$ ionic currents was observed also when temperature increased from 1500 up to 1700 K.

(3) The ratio of intensities of $SnBO_2^+$ and $SnB_2O_4^+$ ionic currents remains constant in time and at the temperature variation. In the case the ionization of $M_2B_2O_4$ molecules (M is an alkali metal) processes of direct [Eq. (10)] and dissociative ionization [Eq. (11)] occur [7]. Ions $M_2BO_2^+$ are formed upon the dissociative ionization of $M_2B_2O_4$ molecules and the electroneutral particle BO_2 is split off.

$$M_2B_2O_4 + e^- = M_2B_2O_4^+ + 2e^-, \quad (10)$$

$$M_2B_2O_4 + e^- = M_2BO_2^+ + BO_2 + 2e^-. \quad (11)$$

The above-stated allows us to claim reliably that only SnB_2O_4 and $Sn_2B_2O_5$ molecules are present in vapor above the $SnO_2–B_2O_3$ system in the temperature range 1300–1500 K at a constant ratio of intensities of $SnBO_2^+$ and $SnB_2O_4^+$ ionic currents. The $SnB_2O_4^+$ ion is a product of SnB_2O_4 direct ionization, and the $SnBO_2^+$ ion is a product of the dissociative ionization of the SnB_2O_4 molecule [Eq. (8)]. A long-term evaporation of the mixture and an increase in temperature result in the appearance of $SnBO_2$ molecules in vapor. As a result of ionization of these molecules [Eq. (8)] and of simultaneous reaction (8) the values of $SnBO_2^+$ ionic currents are summed up. The $Sn_2B_2O_5^+$ ion is a product of the $Sn_2B_2O_5$ direct ionization, and the $Sn_2B_2O_3^+$ is a product of the $Sn_2B_2O_5$ molecule dissociative ionization [Eq. (11)]. Values of ionization energies of the $Sn_2B_2O_4$ and $Sn_2B_2O_5$ molecules calculated by quantum-chemical methods are presented in Table 1. The ionization energies were calculated by the Hartree-Fock method using the Coopmans theorem, by the DFT M06 method [25] (as differences of total

energies of a cation and a neutral particle), and by the Green functions method [26].

To determine equilibrium constants of gas-phase reactions (12)–(15) involving tin borates, in the calculation of the SnB_2O_4 partial pressure we summed up intensities of ionic currents of the $SnBO_2^+$ and $SnB_2O_4^+$ ions, and in the calculation of the $Sn_2B_2O_5$ partial pressure, the intensities of $Sn_2B_2O_3^+$ and $Sn_2B_2O_5^+$ ionic currents.

$$SnO(gas) + B_2O_3(gas) = SnB_2O_4(gas), \quad (12)$$

$$2SnO(gas) + B_2O_3(gas) = Sn_2B_2O_5(gas), \quad (13)$$

$$1/2Sn_2O_2(gas) + B_2O_3(gas) = SnB_2O_4(gas), \quad (14)$$

$$Sn_2O_2(gas) + B_2O_3(gas) = Sn_2B_2O_5(gas). \quad (15)$$

Partial pressures of vapor molecular species were determined by the method of comparing ionic currents, using silver as the pressure standards. [27]. To determine enthalpies of reactions (12)–(15) by Eq. (4) and to reduce enthalpies of reaction (12) calculated by Eq. (5) to the temperature 298 K, we took thermodynamic functions for the gaseous molecules B_2O_3 and SnO from the handbook [19]. Thermodynamic functions of the gaseous oxides Sn_2O_2, SnB_2O_4, and $Sn_2B_2O_5$ were calculated by statistical thermodynamics methods in the approximation rigid rotator-harmonic oscillator. The molecular parameters necessary for this calculation were found by quantum-chemical calculations. Partial pressures of vapor above the system SnO_2–B_2O_3 and the enthalpies of reactions (12)–(15) at 0 K are presented in Tables 3 and 4. The temperature range of calculating equilibrium constants of reaction (12) by Eq. (5) was 1269–1357 K. The value of the reaction (12) enthalpy for the medium of the temperature range 1313 K was –343±20 kJ, and –351±20 kJ when reduced to 298 K.

Tin molybdates. Mixtures of SnO_2 with MoO_3 were evaporated from a molybdenum cell. In the mass spectrum of vapor above the mixture under study in the temperatures range of 1200-1400 K peaks of the ions Sn^+, SnO^+, $Sn_2O_2^+$, $SnMoO_4^+$, $Sn_2MoO_5^+$, $SnMo_2O_7^+$, MoO_2^+, MoO_3^+, $Mo_2O_6^+$, and $Mo_3O_9^+$ were detected. The ratio of ionic current intensities depended on the vaporization time and temperature. As the volatility of molybdenum oxide is higher than that of tin oxide, the condensed phase was gradually depleted of molybdenum oxide, ionic currents of MoO_2^+, MoO_3^+, $Mo_2O_6^+$, and $Mo_3O_9^+$ decreased, and those of Sn^+, SnO^+, and $Sn_2O_2^+$ increased.

Appearance energies of ions in the mass spectrum, eV, are as follows: 15.1±0.4 (Sn^+), 10.6±0.2 (SnO^+), 10±1 ($Sn_2O_2^+$), 11.3±0.3 ($SnMoO_4^+$), 10.0±0.5 ($Sn_2MoO_5^+$), 11.5±0.5 ($SnMo_2O_7^+$), 20±1 (MoO_2^+), 11.9±0.5 (MoO_3^+), 12.0±0.3 ($Mo_2O_6^+$), and 12.0±0.3 ($Mo_3O_9^+$). Appearance energies of the molecular ions SnO^+, MoO_3^+, $Mo_2O_6^+$, and $Mo_3O_9^+$ coincide with ionization energies of corresponding molecules within limits of experimental errors [6, 13]. The appearance energy of Sn^+ exceeds the ionization energy of monatomic tin by 3.6 eV [13]. No breaks were observed in the curve of Sn^+ ionization effectiveness, and ratios of intensities of Sn^+ and SnO^+ ionic currents in the mass spectra of vapor above the studied mixture and above individual tin oxide were equal, which shows that the ion Sn^+ is a product of the molecule SnO dissociative ionization, and the MoO_2^+ ion is a product of dissociative ionization, as its appearance energy exceeds the ionization energy of MoO_2 by 10 eV. Ionization energies of Sn_2O_2, $SnMoO_4$, Sn_2MoO_5, and $SnMo_2O_7$ were calculated by quantum-chemical methods [25, 26]. The resulting data are presented in Table 1. They agree well with the experimental values of appearance energies of the $Sn_2O_2^+$, $SnMoO_4^+$, $Sn_2MoO_5^+$, and $SnMo_2O_7^+$ ions that prove their origination from direct ionization.

To determine standard enthalpies of formation of gaseous tin molybdates, we have measured equilibrium constants of reactions (16)–(36). Partial vapor pressures of molecular species were determined by the method of comparing ionic currents, using gold as the pressure standard [16].

$$SnO(gas) + MoO_3(gas) = SnMoO_4(gas), \quad (16)$$

$$0.5Sn_2O_2(gas) + MoO_3(gas) = SnMoO_4(gas), \quad (17)$$

$$SnO(gas) + 1/2Mo_2O_6(gas) = SnMoO_4(gas), \quad (18)$$

$$1/2Sn_2O_2(gas) + 1/2Mo_2O_6(gas) = SnMoO_4(gas), \quad (19)$$

$$SnO(gas) + 1/3Mo_3O_9(gas) = SnMoO_4(gas), \quad (20)$$

$$1/2Sn_2O_2(gas) + 1/3Mo_3O_9(gas) = SnMoO_4(gas), \quad (21)$$

$$2SnO(gas) + MoO_3(gas) = Sn_2MoO_5(gas), \quad (22)$$

$$Sn_2O_2(gas) + MoO_3(gas) = Sn_2MoO_5(gas), \quad (23)$$

$$SnMoO_4(gas) + SnO(gas) = Sn_2MoO_5(gas), \quad (24)$$

$$SnMoO_4(gas) + 1/2Sn_2O_2(gas) = Sn_2MoO_5(gas), \quad (25)$$

$$2SnO(gas) + 1/2Mo_2O_6(gas) = Sn_2MoO_5(gas), \quad (26)$$

$$Sn_2O_2(gas) + 1/2Mo_2O_6(gas) = Sn_2MoO_5(gas), \quad (27)$$

$$2SnO(gas) + 1/3Mo_3O_9(gas) = Sn_2MoO_5(gas), \quad (28)$$

Table 3. Partial pressures of vapor molecular species and enthalpies of gas-phase reactions (12) and (14) involving SnB_2O_4

T, K	p_i, atm				$-\Delta_r H^0$(0 K), kJ	
	SnO ($\times10^{-5}$)	Sn_2O_2 ($\times10^{-5}$)	B_2O_3 ($\times10^{-7}$)	SnB_2O_4 ($\times10^{-5}$)	reaction (12)	reaction (14)
1350	9.1	–	4.8	2.1	338.8	–
1340	5.4	–	1.6	1.5	350.8	–
1347	4.6	–	4.0	1.2	342.0	–
1343	2.7	–	4.0	0.5	337.2	–
1358	15.8	14.0	2.3	3.0	347.0	205.3
1369	23.9	13.3	4.3	2.9	337.5	199.6
1362	19.2	6.2	4.9	2.5	334.9	199.7
1362	14.7	6.2	4.3	2.1	337.6	199.3
1363	14.7	3.7	5.2	1.9	334.4	198.9
1364	13.6	3.7	5.3	1.7	334.3	197.7
1366	11.7	2.5	5.3	1.4	334.3	198.2
1367	9.8	2.2	4.3	1.2	336.8	199.2
1367	9.1	1.5	4.9	1.0	334.0	197.8
1366	7.9	1.4	4.6	0.9	335.0	197.6
1365	7.2	0.9	4.9	0.7	332.0	196.1
1365	5.3	0.8	3.6	0.6	337.7	198.9
1363	5.3	0.5	4.3	0.5	332.3	196.6
1363	4.2	0.6	3.3	0.4	336.4	197.4
1362	3.8	0.4	3.9	0.4	333.5	195.7
1383	4.2	0.4	5.0	0.5	338.3	198.6
1381	4.0	0.3	5.3	0.4	334.9	196.7
1381	3.3	0.3	4.7	0.3	336.4	196.1
1381	3.4	0.3	5.0	0.3	335.3	196.2
1380	3.2	0.2	4.3	0.3	336.8	197.6
1379	3.2	0.2	4.3	0.2	334.6	196.1
1378	2.9	0.2	4.3	0.2	335.7	196.7
1378	2.9	0.2	5.0	0.2	334.1	195.0
1378	2.8	0.2	4.3	0.2	335.3	195.8
1455	27.8	10.9	3.3	2.5	357.6	214.2
1455	43.9	11.2	5.4	3.1	348.8	210.8
1458	55.8	25.1	5.0	4.9	353.2	213.0
1468	57.6	24.3	5.8	4.8	353.0	212.5
1473	53.7	18.5	6.2	4.4	353.1	212.8

Table 3. (Contd.)

T, K	p_i, atm				$-\Delta_r H^0$(0 K), kJ	
	SnO ($\times 10^{-5}$)	Sn_2O_2 ($\times 10^{-5}$)	B_2O_3 ($\times 10^{-7}$)	SnB_2O_4 ($\times 10^{-5}$)	reaction (12)	reaction (14)
1479	50.6	18.6	5.4	4.6	357.5	216.0
1482	49.2	16.7	5.9	4.2	356.4	214.9
1481	46.2	15.7	5.9	4.2	356.9	215.1
1480	44.7	13.7	6.3	3.7	354.8	213.6
1481	40.2	13.7	5.4	3.6	357.6	215.0
1478	40.2	12.1	6.3	3.5	354.8	213.2
1479	37.2	12.7	4.6	3.3	359.1	216.1
1478	35.7	10.4	5.0	3.1	357.7	215.6
1478	32.7	10.4	5.0	3.0	358.5	215.2
1478	32.7	8.2	5.0	2.8	357.4	215.7
1479	26.8	8.2	4.2	2.5	361.2	217.0
1479	26.8	7.2	5.0	2.4	358.1	214.6
1479	23.8	7.2	3.8	2.2	362.3	217.4
1482	23.9	6.2	3.8	2.1	362.4	218.1
1491	22.5	5.9	4.6	2.1	362.6	217.0
1578	61.9	10.4	22.8	7.8	366.4	222.0
1577	52.4	9.4	18.7	5.8	367.0	221.3
1575	49.1	7.0	18.7	5.7	367.2	222.7
1582	41.4	6.6	17.5	4.6	369.1	222.1
1582	33.4	4.3	17.5	4.2	370.8	224.0
1580	31.8	4.2	17.4	3.3	367.9	220.6
1342	7.5	3.4	0.2	0.8	360.8	220.2
1344	5.5	3.4	0.2	0.7	364.0	219.8
1346	4.9	1.2	0.2	0.5	361.3	221.2
1346	3.5	1.3	0.2	1.1	375.2	231.3
1344	3.1	0.3	0.2	0.3	364.1	227.5
1344	2.0	0.3	0.2	0.1	363.8	222.4
1343	2.0	0.5	0.2	0.2	368.4	223.9
1343	1.5	0.5	0.1	0.1	366.8	223.9
1342	1.4	0.2	0.1	0.1	366.5	223.8
1431	3.8	0.6	0.8	0.4	371.5	224.3
1428	3.1	0.2	0.8	0.4	373.0	230.2
1436	1.4	0.2	0.8	0.3	379.8	227.1
1439	1.3	0.1	0.8	0.2	374.8	227.2
				Average value	351.8±14.2	211.1±11.4

Table 4. Partial pressures of vapor molecular species and enthalpies of gas-phase reactions (13) and (15) involving $Sn_2B_2O_5$

T, K	p_i, atm				$-\Delta_r H^0$(0 K), kJ	
	SnO ($\times10^{-5}$)	Sn_2O_2 ($\times10^{-6}$)	B_2O_3 ($\times10^{-7}$)	$Sn_2B_2O_5$ ($\times10^{-6}$)	reaction (13)	reaction (15)
1356	4.2	10.5	2.2	1.6	671.5	388.8
1360	6.0	11.6	3.3	2.0	663.3	386.8
1361	5.6	9.9	3.4	1.8	663.9	387.3
1362	5.4	10.9	3.3	1.6	664.2	385.5
1362	5.1	10.6	3.5	1.6	664.8	385.1
1362	5.0	9.6	3.3	1.5	665.2	386.2
1362	4.8	9.6	3.3	1.4	665.3	385.4
1362	4.8	9.6	3.1	1.3	665.2	385.3
1363	4.5	8.9	3.0	1.2	666.6	385.9
1363	4.4	7.9	3.0	1.2	667.1	387.2
1363	4.1	10.9	3.1	1.0	666.3	381.2
1363	4.1	6.9	3.0	1.0	666.6	386.7
1363	3.8	6.0	3.0	0.9	667.2	387.1
1363	3.6	5.0	2.8	0.8	667.8	388.6
1400	5.3	6.1	5.8	0.9	669.4	389.4
1401	4.8	4.8	6.3	0.8	669.8	390.2
1402	4.5	4.4	6.3	0.6	668.5	388.1
1402	3.9	3.4	5.8	0.6	672.8	392.1
1401	3.9	3.4	5.8	0.4	667.6	387.1
1401	3.6	3.1	5.4	0.4	670.3	389.0
1330	4.0	7.0	0.9	1.5	669.2	395.2
1334	3.9	7.0	0.8	1.5	673.0	397.7
1334	3.7	6.4	0.9	1.5	672.9	397.4
1335	3.5	6.2	0.9	1.5	674.6	398.0
1334	3.4	6.1	0.9	1.5	674.8	397.9
1334	3.3	5.7	0.8	1.3	675.2	398.4
1335	3.2	5.3	0.8	1.2	675.5	398.6
1366	4.5	7.6	1.3	1.4	679.3	399.8
1371	4.3	5.8	1.5	1.1	678.3	399.9
1371	4.0	5.2	1.4	0.8	677.2	398.3
1371	3.3	4.3	1.1	0.7	682.8	401.7
1291	1.5	8.5	0.3	1.4	682.1	392.9

Table 4. (Contd.)

T, K	p_i, atm				$-\Delta_r H^0$(0 K), kJ	
	SnO ($\times10^{-5}$)	Sn_2O_2 ($\times10^{-6}$)	B_2O_3 ($\times10^{-7}$)	$Sn_2B_2O_5$ ($\times10^{-6}$)	reaction (13)	reaction (15)
1314	2.0	6.7	0.3	1.4	687.7	402.3
1317	2.4	7.2	0.6	2.2	682.6	399.8
1317	2.4	6.7	0.7	2.1	680.4	398.4
1317	2.4	5.8	0.6	2.0	681.6	401.1
1318	2.4	5.8	0.6	1.9	681.5	400.9
1317	2.2	5.3	0.6	1.8	682.3	401.0
1316	2.2	4.6	0.5	1.7	683.2	403.6
1314	2.0	4.6	0.5	1.5	682.9	401.6
1314	1.9	4.0	0.5	1.5	684.0	403.1
1346	3.0	5.2	0.9	1.9	686.2	405.8
1345	2.6	4.1	0.8	1.5	687.5	406.9
1345	2.5	4.4	0.9	1.5	687.1	404.8
1345	2.4	3.8	0.8	1.4	688.6	407.0
1344	2.4	3.5	0.8	1.2	686.3	405.9
1344	2.2	3.4	0.6	1.1	690.5	408.4
1343	2.0	3.1	0.6	0.9	689.9	406.9
1343	1.8	2.5	0.5	0.9	694.3	411.4
1343	1.8	2.4	0.6	0.8	690.9	408.5
Average value					676±9	395±8

$$Sn_2O_2(gas) + 1/3Mo_3O_9(gas) = Sn_2MoO_5(gas), \quad (29)$$

$$SnO(gas) + 2MoO_3(gas) = SnMo_2O_7(gas), \quad (30)$$

$$1/2Sn_2O_2(gas) + 2MoO_3(gas) = SnMo_2O_7(gas), \quad (31)$$

$$SnO(gas) + Mo_2O_6(gas) = SnMo_2O_7(gas), \quad (32)$$

$$1/2Sn_2O_2(gas) + Mo_2O_6(gas) = SnMo_2O_7(gas), \quad (33)$$

$$SnO(gas) + 2/3Mo_3O_9(gas) = SnMo_2O_7(gas), \quad (34)$$

$$1/2Sn_2O_2(gas) + 2/3Mo_3O_9(gas) = SnMo_2O_7(gas), \quad (35)$$

$$SnMoO_4(gas) + MoO_3(gas) = SnMo_2O_7(gas). \quad (36)$$

Values of partial pressures of vapor molecular species above the system SnO_2–MoO_3 are presented in Table 5.

Quantum-chemical calculations of structures of gaseous tin salts and of enthalpies of reactions with their participation. Quantum-chemical calculations of structures and energy characteristics of gaseous salts were carried out using two different approaches to the description of many-electron systems and to the calculation of enthalpies of chemical reactions. The first approach [28] is based on the use of the many-electron wave functions explicitly containing interelectronic distances to account correlation effect for intermediate values of these distances. Such approaches include a set of methods entitled "explicitly correlated" or F12 methods [29–33]. These methods are realized in the program MOLPRO [34] using the variational perturbation theory (MP2–F12) [35] and the method of the coupled clusters [CCSD (T)-F12] [36].

The second approach uses a reduced electronic density matrix (function) of the first order and includes methods of the so-called density functional theory (DFT). Enthalpies of reactions involving gaseous tin

Table 5. Partial pressures of vapor molecular species above the SnO_2–MoO_3 system

T, K	p_i, atm								
	SnO ($\times10^{-6}$)	Sn_2O_2 ($\times10^{-6}$)	MoO_2 ($\times10^{-6}$)	MoO_3 ($\times10^{-7}$)	Mo_2O_6 ($\times10^{-5}$)	Mo_3O_9 ($\times10^{-5}$)	$SnMoO_4$ ($\times10^{-6}$)	Sn_2MoO_5 ($\times10^{-6}$)	$SnMo_2O_7$ ($\times10^{-5}$)
1231	0.23	2.68	1.53	5.46	0.45	2.15	0.51	0.85	0.76
1233	0.23	3.04	1.67	5.08	0.51	2.05	0.51	0.71	1.00
1236	0.23	2.51	1.54	4.70	0.42	1.95	0.34	0.57	0.99
1360	1.70	4.34	2.15	8.19	0.93	3.05	2.18	1.02	1.84
1353	1.82	5.69	2.29	6.86	0.73	2.02	2.17	1.09	2.08
1355	2.15	4.91	1.68	5.15	0.89	1.80	2.79	1.05	2.03
1356	1.99	4.72	1.53	5.16	0.56	1.46	2.02	0.86	2.24
1357	1.66	3.74	1.38	3.87	0.56	1.46	2.48	0.82	1.56
1358	1.49	3.35	1.24	3.01	0.46	1.13	1.55	0.74	1.52
1359	1.40	2.95	0.97	2.58	0.43	1.02	1.03	0.62	1.29
1325	2.40	12.63	2.71	11.51	4.08	14.29	8.47	7.99	9.48
1332	2.05	12.69	2.72	8.49	3.75	9.63	7.27	8.03	8.79
1334	1.61	9.89	1.90	4.64	4.11	9.47	7.03	6.13	9.18
1336	1.61	9.90	1.74	5.80	2.86	6.75	6.03	6.14	8.08
1339	1.53	9.57	1.33	5.12	2.87	7.31	7.81	5.38	9.36
1341	1.26	8.88	1.33	4.19	2.52	7.50	5.80	6.93	7.58
1344	1.26	9.25	1.00	3.74	3.06	7.34	7.84	5.02	8.35
1345	1.17	8.19	1.00	3.51	2.10	5.32	6.32	5.79	6.34
1346	1.26	7.13	0.67	2.81	1.98	5.69	7.85	4.64	7.32
1345	1.26	6.77	0.75	2.57	1.38	3.67	4.81	3.86	4.47
1335	4.00	13.50	3.00	2.59	4.87	7.81	8.19	5.62	6.92
1336	3.75	12.52	4.62	17.30	3.90	5.77	8.19	3.96	6.88
1337	2.75	9.23	2.47	6.06	3.34	5.78	6.56	10.37	3.65
1338	2.51	7.26	2.55	5.41	2.37	3.74	6.56	2.18	4.45
1340	1.67	6.28	1.08	3.47	1.95	3.92	4.70	1.92	3.35
1340	2.26	5.29	1.47	3.04	1.81	2.90	6.10	2.18	3.18
1342	1.68	3.31	0.74	2.39	1.72	3.07	4.70	1.00	3.40
1344	1.93	6.63	0.77	2.39	0.93	1.82	3.53	1.62	3.07
1345	1.85	5.97	0.61	2.18	1.17	1.82	5.18	2.06	4.03
1344	1.85	3.08	0.60	1.74	1.17	1.59	5.18	1.08	3.28
1346	1.51	2.69	0.37	1.16	0.98	1.65	3.38	1.20	3.15
1346	1.18	2.59	0.47	1.31	0.93	1.48	3.14	0.58	1.75

Table 5. (Contd.)

T, K	p_i, atm								
	SnO ($\times10^{-6}$)	Sn_2O_2 ($\times10^{-6}$)	MoO_2 ($\times10^{-6}$)	MoO_3 ($\times10^{-7}$)	Mo_2O_6 ($\times10^{-5}$)	Mo_3O_9 ($\times10^{-5}$)	$SnMoO_4$ ($\times10^{-6}$)	Sn_2MoO_5 ($\times10^{-6}$)	$SnMo_2O_7$ ($\times10^{-5}$)
1348	1.18	2.09	0.40	0.65	0.89	1.43	3.86	0.62	1.75
1274	0.87	5.39	2.27	5.09	3.71	5.55	2.76	9.15	5.41
1273	2.45	4.09	2.12	3.96	1.63	2.66	1.73	3.53	3.17
1273	0.55	3.23	1.11	3.11	1.31	2.89	1.43	4.14	2.87
1274	0.38	2.59	1.06	2.40	1.13	2.22	1.17	3.05	1.80
1273	0.46	2.58	0.86	1.55	1.02	2.11	1.38	3.05	2.03
1276	0.52	2.37	0.91	2.27	1.02	1.56	1.38	2.81	1.91
1276	0.49	1.94	0.81	1.84	0.80	1.56	1.28	1.95	1.87
1277	0.46	2.07	0.76	2.13	0.87	1.41	1.07	2.20	1.31
1277	0.44	1.75	0.66	1.56	0.84	1.41	1.18	2.20	1.54
1277	0.44	2.14	0.66	1.56	0.84	1.30	0.97	1.83	1.58
1278	0.44	1.43	0.53	1.42	0.77	1.30	1.13	1.71	1.37
1275	0.44	1.42	0.53	1.84	0.62	1.00	1.02	1.46	1.25
1274	0.41	1.55	0.47	1.70	0.55	0.93	0.97	1.46	0.87
1275	0.34	1.29	0.47	1.13	0.51	0.96	0.97	1.10	1.07
1278	0.38	1.04	0.30	0.85	0.47	0.96	0.87	1.43	1.03
1379	2.83	4.66	0.98	1.68	1.73	2.65	5.30	5.68	4.43

salts were calculated by the MP2-F12 method using the MOLPRO software and by the DFTM06 method [26] using the GAUSSIAN'09 software [37]. For all atoms the Gaussian Def2-TZVP basis set [38] was taken, for tin and molybdenum atoms with the corresponding effective core potentials. The search for equilibrium geometries and the calculation of frequencies of harmonic vibrations were carried out by the DFTM06 method. Resulting structures of all isomers were checked by optimization using the standard MP2 method with subsequent calculation of normal mode frequencies. Geometrical structures and vibrational spectra of all studied molecules were visualized using Chemcraft [39] and Avogadro [40] graphical programs.

Resulting structural isomers of gaseous tin borates are presented in Fig. 1. For the SnB_2O_4 molecules structure **I** has the least energy. The energy of the molecule with structure **II** is higher by 58 kJ. Hereinafter differences in energies of structural isomers were determined in view of correction for the energy of zero vibrations. Structure **III** of the $Sn_2B_2O_5$ molecule is the least in energy among presented structures. Structures **IV** and **V** are higher in energy than structure **III** by 24 and 98 kJ, respectively.

Structures of gaseous tin molybdates $SnMoO_4$, $SnMo_2O_7$, and Sn_2MoO_5 are presented in Fig. 2. In the case of the $SnMoO_4$ molecule structure **I** with the C_{2v} symmetry typical for the majority of gaseous MXO_4 molybdates [9] (M is a metal of the 2nd or 14th group of the periodic system or a 3*d*-element) has the minimal energy. Structure **II** is higher in energy by 130 kJ. Structures **III** and **V** for the $SnMo_2O_7$ and Sn_2MoO_5 molecules are energy favorable. Structures **IV** and **VI** are higher in energy by 250 and 15 kJ, respectively. Structure **V** was not considered in [4], and structure **VI** was accepted as the minimal in energy.

Structural isomers of gaseous tin vanadate are presented in Fig. 3. The tin atom can move in the plane passing through oxygen atoms designated in Fig. 3 as

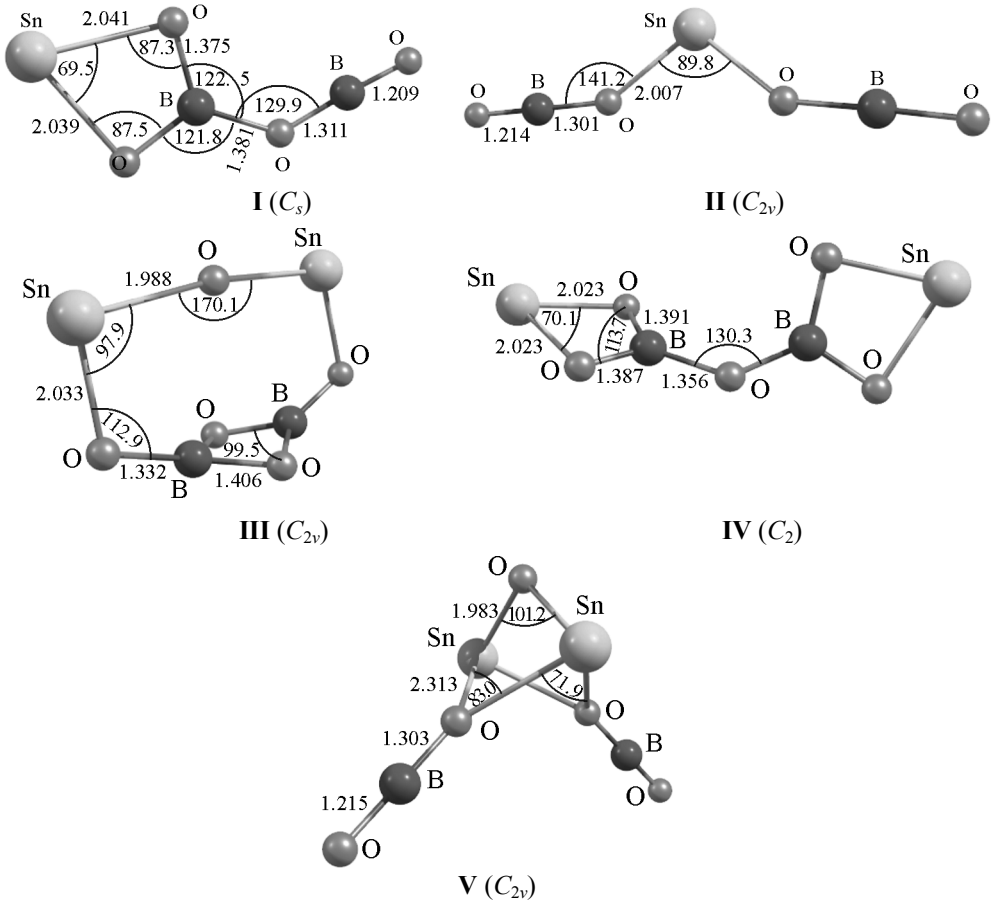

Fig. 1. Probable structures **I–V** of gaseous tin borates.

O_3 and O_4 and through the bisecting point of the segment connecting vanadium atoms. The symmetry of structure **I** in this case is reduced to C_s. Differences in energies and structural characteristics of these enantiomers are negligible, therefore structures **II** and **III** were not considered in the calculation of thermodynamic functions.

Enthalpies of reactions involving gaseous tin salts are presented in Table 6.

The resulting enthalpies of reactions (5), (6), (12)–(15), (16)–(36) reduced to 298 K in combination with enthalpies of formation of the gaseous oxides of tin SnO (21.9±4.0 [19]), Sn_2O_2 (–238.5±25.1 [6]), vanadium V_4O_{10} (–2825±40 [19]), boron B_2O_3 (–835.4±8.1 [19]), and molybdenum MoO_3 (–364.4±15.1 [19]), Mo_2O_6 (–1149.4±40 [19]) and Mo_3O_9 (–1902.0±40 [19]) have allowed us to find standard formation enthalpies of gaseous tin vanadate, borates, and molybdates (Table 7).

The consideration of atomization enthalpy variation in isoanion and isocation groups of gaseous salts M_mXO_n (M is cation-, X is anion-forming element, m = 1, 2) clearly show linear dependence (37) of $\Delta_{at}H^0$ of salts on the atomization enthalpy of gaseous anion-forming oxides.

$$\Delta_{at}H^0(\text{salt, gas, 298 K}) = k\Delta_{at}H^0(\text{anion-forming oxide, gas, 298 K}) + b. \quad (37)$$

The values of formation and atomization enthalpies of the gaseous molecules SnV_2O_6, SnB_2O_4, $Sn_2B_2O_5$, $SnMoO_4$, Sn_2MoO_5, and $SnMo_2O_7$ found in this work in combination with published atomization enthalpies of the gaseous molecules $SnPO_2$, $SnPO_3$ [2], $SnWO_4$, Sn_2WO_5, and SnW_2O_7 [3] allow us to obtain such a dependence for the isocation series of gaseous tin salts (Fig. 4). Straight line *1* (m = 1) shows the dependence for salts with one tin atom, and straight line *2* (m = 2) characterizes the dependence for salts containing two tin atoms. As thermodynamic functions of gaseous tin tungstates were only estimated in [3] dedicated to the determination of formation enthalpies of these salts, in [4] thermodynamic functions of the salts $SnWO_4$, Sn_2WO_5, SnW_2O_7 were calculated by the quantum-

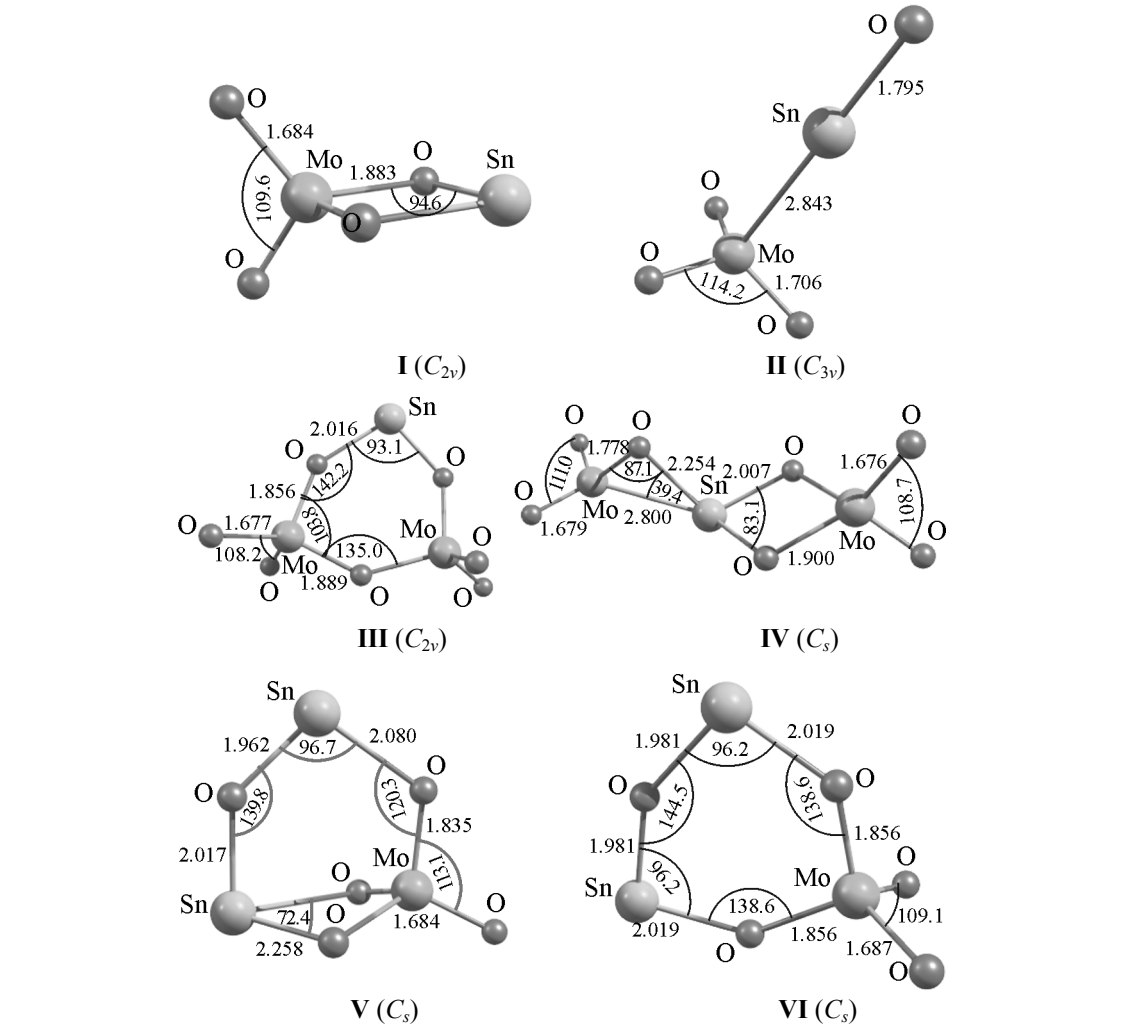

Fig. 2. Probable structures **I–VI** of gaseous tin molybdates.

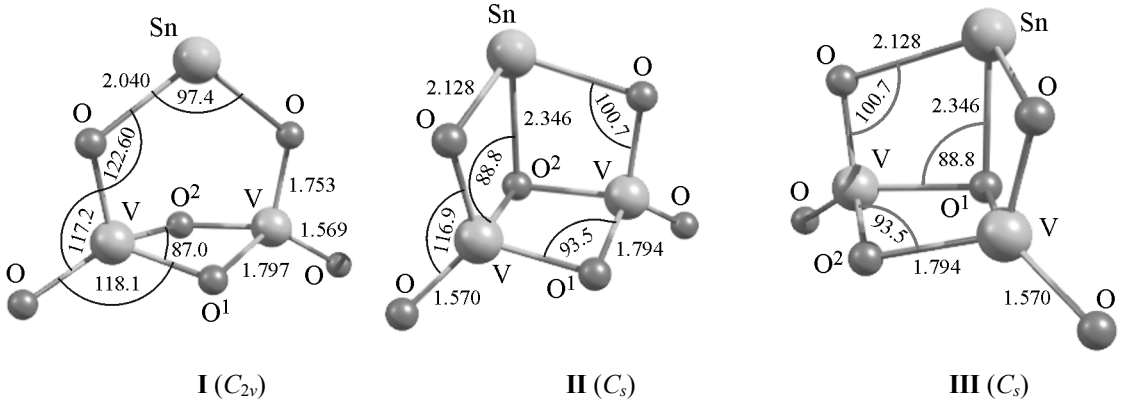

Fig. 3. Structure of gaseous tin vanadate **I** and its enantiomers **II, III**.

Table 6. Experimental and calculated by quantum-chemical methods values of enthalpies of reactions (6), (7), (12)–(15), (16)–(36)[a]

Reaction	$-\Delta_r H^0$(0 K), kJ			
	quantum-chemical calculations, method			experimental
	DFT M06	MP2	MP2+f12	
$SnO(^1\Sigma^+) + 1/2V_4O_{10}(^1A_1) = SnV_2O_6(^1A_1)$	144	100	103	134±5
$Sn_2O_2(^1A_g) + V_4O_{10}(^1A_1) = 2\ SnV_2O_6(^1A_1)$	–13	–8	–4	–38±5
$SnO(^1\Sigma^+) + B_2O_3(^1A_1) = SnB_2O_4(^1A')$	322	304	296	352±14
$1/2Sn_2O_2(^1A_g) + B_2O_3(^1A_1) = SnB_2O_4(^1A')$	171	121	119	211±11
$2\ SnO(^1\Sigma^+) + B_2O_3(^1A_1) = Sn_2B_2O_5(^1A)$	614	574	557	676±9
$Sn_2O_2(^1A_g) + B_2O_3(^1A_1) = Sn_2B_2O_5(^1A)$	312	303	287	395±8
$SnO(^1\Sigma^+) + MoO_3(^1A_1) = SnMoO_4(^1A_1)$	428	353	370	368±13
$1/2Sn_2O_2(^1A_g) + MoO_3(^1A_1) = SnMoO_4(^1A_1)$	277	225	237	195±13
$SnO(^1\Sigma^+) + 1/2Mo_2O_6(^1A_g) = SnMoO_4(^1A_1)$	202	149	154	163±6
$1/2Sn_2O_2(^1A_g) + 1/2Mo_2O_6(^1A_g) = SnMoO_4(^1A_1)$	51	21	22	–9±5
$SnO(^1\Sigma^+) + 1/3Mo_3O_9\ (^1A_1') = SnMoO_4(^1A_1)$	142	87	95	110±5
$1/2Sn_2O_2(^1A_g) + 1/3Mo_3O_9\ (^1A_1') = SnMoO_4(^1A_1)$	–9	–40	–37	–62±5
$2SnO(^1\Sigma^+) + MoO_3(^1A_1) = Sn_2MoO_5(^1A')$	738	614	638	707±14
$Sn_2O_2(^1A_g) + MoO_3\ (^1A_1) = Sn_2MoO_5(^1A')$	437	359	373	363±12
$SnO(^1\Sigma^+) + SnMoO_4\ (^1A_1) = Sn_2MoO_5(^1A')$	310	261	268	340±8
$1/2Sn_2O_2(^1A_g) + SnMoO_4\ (^1A_1) = Sn_2MoO_5(^1A')$	159	134	136	167±7
$2SnO(^1\Sigma^+) + 1/2Mo_2O_6(^1A_g) = Sn_2MoO_5(^1A')$	513	411	496	503±9
$Sn_2O_2(^1A_g) + 1/2Mo_2O_6(^1A_g) = Sn_2MoO_5(^1A')$	211	155	158	1596
$2SnO(^1\Sigma^+) + 1/3Mo_3O_9\ (^1A_1') = Sn_2MoO_5(^1A')$	453	348	363	450±9
$Sn_2O_2(^1A_g) + 1/3Mo_3O_9(^1A_1') = Sn_2MoO_5(^1A')$	151	93	98	106±6
$SnO(^1\Sigma^+) + Mo_2O_6(^1A_g) = SnMo_2O_7(^1A_1)$	360	292	291	324±7
$1/2Sn_2O_2(^1A_g) + Mo_2O_6(^1A_g) = SnMo_2O_7(^1A_1)$	209	165	159	227±8
$SnO(^1\Sigma^+) + 2/3Mo_3O_9(^1A_1') = SnMo_2O_7(^1A_1)$	240	168	172	218±5
$1/2Sn_2O_2(^1A_g) + 2/3Mo_3O_9(^1A_1') = SnMo_2O_7(^1A_1)$	89	41	40	46±4
$SnO(^1\Sigma^+) + 2MoO_3(^1A_1) = SnMo_2O_7(^1A_1)$	811	699	722	732±21
$1/2Sn_2O_2(^1A_g) + 2MoO_3(^1A_1) = SnMo_2O_7(^1A_1)$	660	571	589	635±22
$SnMoO_4(^1A_1) + MoO_3(^1A_1) = SnMo_2O_7(^1A_1)$	383	346	352	365±9

[a] Symbols in parentheses designate terms of ground states of molecules.

chemistry method and their formation enthalpies were corrected.

For the tin salts with $m = 1$ coefficients k and b are equal to 0.992±0.015 and 902.2±39.9, respectively, and the correlation coefficient is 0.9994. For the tin salts with $m = 2$ coefficients k and b are 0.982±0.089 and 1798.6±193.7, respectively, and the correlation coefficient is 0.9959.

The value of atomization enthalpy of gaseous tin vanadate is not shown in Fig. 4 because the value of

Table 7. Enthalpies of reactions (6), (7), (12)–(15), (16)–(36) and standard enthalpies of formation of gaseous tin salts

Gas-phase reaction	$-\Delta_r H^0$ (298 K), kJ	$-\Delta_f H^0$ (salt, 298 K, gas), kJ/mol	Recommended value of $-\Delta_f H^0$(salt, 298 K, gas), kJ/mol
$SnO + 1/2V_4O_{10} = SnV_2O_6$	133±8	1524±22	1520±24
$Sn_2O_2 + V_4O_{10} = 2\ SnV_2O_6$	–33±10	1515±24	
$SnO + B_2O_3 = SnB_2O_4$	353±20	1168±17	1166±22
$1/2Sn_2O_2 + B_2O_3 = SnB_2O_4$	212±11	1164±22	
$2SnO + B_2O_3 = Sn_2B_2O_5$	682±9	1474±13	1476±28
$Sn_2O_2 + B_2O_3 = Sn_2B_2O_5$	405±8	1479±28	
$SnO + MoO_3 = SnMoO_4$	366±13	709±20	699±29
$1/2Sn_2O_2 + MoO_3 = SnMoO_4$	194±13	678±27	
$SnO + 1/2Mo_2O_6 = SnMoO_4$	161±6	714±29	
$1/2Sn_2O_2 + 1/2Mo_2O_6 = SnMoO_4$	–8±5	686±34	
$SnO + 1/3Mo_3O_9 = SnMoO_4$	107±5	719±24	
$1/2Sn_2O_2 + 1/3Mo_3O_9 = SnMoO_4$	–63±3	690±29	
$2SnO + MoO_3 = Sn_2MoO_5$	704±14	1025±21	1001±38
$Sn_2O_2 + MoO_3 = Sn_2MoO_5$	363±12	966±32	
$SnMoO_4 + SnO = Sn_2MoO_5$	339±8	1016±30	
$SnMoO_4 + 1/2Sn_2O_2 = Sn_2MoO_5$	166±7	984±35	
$2\ SnO + 1/2Mo_2O_6 = Sn_2MoO_5$	500±9	1031±30	
$Sn_2O_2 + 1/2Mo_2O_6 = Sn_2MoO_5$	159±6	972±38	
$2\ SnO + 1/3Mo_3O_9 = Sn_2MoO_5$	447±9	1037±25	
$Sn_2O_2 + 1/3Mo_3O_9 = Sn_2MoO_5$	105±6	978±35	
$SnO + Mo_2O_6 = SnMo_2O_7$	324±7	1452±41	1456±60
$1/2Sn_2O_2 + Mo_2O_6 = SnMo_2O_7$	228±8	1497±44	
$SnO + 2/3Mo_3O_9 = SnMo_2O_7$	216±5	1462±33	
$1/2Sn_2O_2 + 2/3Mo_3O_9 = SnMo_2O_7$	46±4	1433±37	
$SnO + 2\ MoO_3 = SnMo_2O_7$	731±21	1438±60	
$1/2Sn_2O_2 + 2\ MoO_3 = SnMo_2O_7$	635±22	1483±35	
$SnMoO_4 + MoO_3 = SnMo_2O_7$	366±9	1429±34	

the formation enthalpy of the anion-forming oxide V_2O_5(gas) lacks in the literature. Equations (37) deduced for tin (m = 1) and lead salts [8, 41, 42] allow us to estimate the formation enthalpy of the oxide V_2O_5 (–1170 kJ/mol).

Gaseous tin salts are a convenient object for revealing general regularities characteristic of gaseous inorganic associates. A clear analogy is traced in properties of salts of oxygen-containing acids and associates, which are traditionally referred to in the literature as complex halides.

The study of structures of gaseous M_mXO_n salts and complex halides M_mXHlg_n has shown that in all cases the structure, interatomic distances, angles, and normal mode frequencies of structurally rigid anionic groups (XO_n and $XHlg_n$) are independent of the nature of a metal atom M. This latter, in turn, is mobile, and we can consider only its most probable location

corresponding to a global minimum on the molecule potential energy surface. In cases of isolated molecules of salts of oxygen-containing acids and of complex halides, both experiments and quantum-chemical calculations confirm the concept of their structurally nonrigid configurations including free motion of a metal atom around an "anionic" group of atoms.

The structure of complex halides $M^{I}X^{III}Hlg_4$ and $M^{I}X^{II}Hlg_3$ (Roman numbers show oxidation states of M and X) completely coincides with the structure of salts of oxygen-containing acids of analogous composition, for example, perrhenates and phosphates of alkali metals $MReO_4$ [43] and MPO_3 [44], respectively.

Formation of di-, tri-, and even tetramers is typical of gaseous halides. In this connection complex halides with the following mole proportions of halide components 1 : 1 ($LiGaF_4$), 1 : 2 ($NaSn_2F_5$), 2 : 1 (Li_2GaF_5), and 2 : 2 ($Li_2Ga_2F_8$) were detected in saturated vapor above binary halide systems [45].

In the vapor above the individual oxides SnO_2 and MoO_3 oligomers are also present [5]. Therefore salts with mole proportions of the constituent oxides SnO and MoO_3 1 : 1 ($SnMoO_4$), 1 : 2 ($SnMo_2O_7$), and 2 : 1 (Sn_2MoO_5) are present in vapor above the system SnO_2–MoO_3. We did not find the associate with composition 2 : 2 ($Sn_2Mo_2O_{8)}$, though existence of the tin tungstate $Sn_2W_2O_8$ is known [3]. The lead oxide PbO is also polymerized in vapor [5]. Therefore in the saturated vapor above the systems PbO–MoO_3 and PbO–WO_3 there are gaseous salts with various ratios of PbO and MoO_3 (WO_3) oxides.

In vapor above B_2O_3 only monomer [5] was detected. That is why borates with the mole ratios 1 : 2 or 2 : 2 of the oxides SnO–B_2O_3 are present in the saturated vapor above the system SnO_2–B_2O_3.

As a number of regularities determining criteria of thermal stability [10], connections of atomization enthalpies of salts with atomization enthalpies of cation- and anion-forming oxides were revealed for gaseous salts of oxygen-containing acids, it is hoped that these regularities are also valid for complex halides. Complex halides, which should be named salts of halogen-containing acids, can be presented similarly to salts of oxygen-containing acids as products of reactions between basic and acid halides.

Taking into consideration pronounced structural similarity of gaseous salts of oxygen-containing acids and complex halides, we might expect that Eqs. (37) deduced for complex halides forming isocation series make it possible to estimate atomization enthalpies and to calculate formation enthalpies of yet unstudied compounds and also to correct experimental data, which are falling outside the limits of linear dependences.

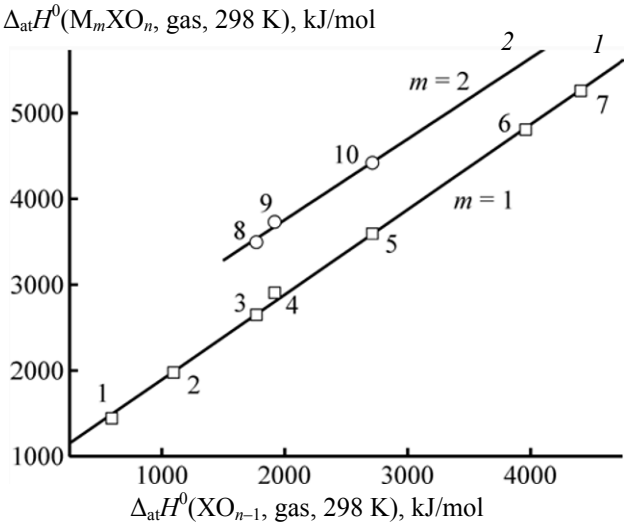

Fig. 4. Dependence of atomization enthalpy of gaseous tin salts on the atomization enthalpy of gaseous anion-forming oxides. (*1*) m = 1: (1) $SnPO_2$, (2) $SnPO_3$, (3) $SnMoO_4$, (4) $SnWO_4$, (5) SnB_2O_4, (6) $SnMo_2O_7$, (7) SnW_2O_7; (*2*) m = 2: (8) Sn_2MoO_5, (9) Sn_2WO_5, (10) $Sn_2B_2O_5$.

EXPERIMENTAL

The study was carried out on an MS-1301 mass spectrometer at the ionizing voltage of 30 eV. Mixtures of the oxides [SnO_2 + MoO_3] and [SnO_2 + B_2O_3] were evaporated from a molybdenum cell heated by a resistance furnace. Temperature was measured by a platinum–platinum-rhodium thermocouple. A mixture of [SnO_2 + V_2O_5] was evaporated from an effusion cell made of zirconium dioxide. The cell was heated up by electronic bombing, temperature was measured by an EOP-66 optical pyrometer.

Partial pressures of vapor components were determined by the method of comparing ionic currents using Eq. (38). Silver [27] or gold [16] were used as pressure standards.

$$p_i = p_s \frac{I_i T_i \sigma_s \gamma_s}{I_s T_s \sigma_i \gamma_i}. \qquad (38)$$

Here p is a partial pressure of a vapor component, I is the ionic current intensity, T is temperature (K), σ is ionization cross-sections of a molecule, γ is the

conversion ratio of the secondary electron multiplier of the mass-spectrometer, indexes *i* and *s* refer to a substance under study and a standard, respectively.

Ionization cross-sections of molecules were calculated by the additivity method using values of atomic cross-sections [17]. A correcting coefficient 0.7 was applied in the calculation of ionization cross-sections of gaseous tin salts with V_4O_{10} [18].

To determine vapor molecular composition, we measured appearance energies of ions in mass spectra by the method of disappearing ionic current, using values of gold ionization energies as a standard [13]. The instrumentation was preliminarily calibrated against vapor pressure of CaF_2 [19].

ACKNOWLEDGMENTS

This work was fulfilled using the inventory of the "Computer resource center" of St. Petersburg State University.

REFERENCES

1. Lopatin, S.I., Gunina, A.O., and Shugurov, S.M., *Russ. J. Gen. Chem*., 2011, vol. 81, no. 10, p. 2045. DOI: 10.1134/S1070363211100021.
2. Lopatin, S.I. and Semenov, G.A., *Russ. J. Gen. Chem*., 1996, vol. 66, no. 2, p. 170.
3. Bulova, M.N., Alikhan'an, A.S., and Gas'rov, A.M., *Neorg. Mater*., 2002, vol. 38, no. 7, p. 688. DOI: 10.1023/A:1016240425105.
4. Lopatin, S.I. and Shugurov, S.M., *Russ. J. Gen. Chem*. 2008, vol. 78, no. 5, p. 847. DOI: 10.1134/S1070363208050010.
5. Kazenas, E.K. and Tsvetkov, Yu.V., *Isparenie oksidov* (Vaporization of Oxides), Moscow: Nauka, 1997.
6. Colin, R., Drowart, J., and Verhaegen, G., *Trans. Faraday Soc*., 1965, vol. 61, no. 511, pt. 7, p. 1364.
7. Lopatin, S.I. and Stolyarova, V.L., *Glass Phys. Chem*., 2006, vol. 32, no. 3, p. 353. DOI: 10.1134/S1087659606030163.
8. Lopatin, S.I., Mittova, I.J., Gerasimov, F.S., Shugurov, S.M., Kostryukov, V.F., and Skorokhodova, S.M., *Russ. J. Inorg. Chem*, 2006, vol. 51, no. 10, p. 1646. DOI: 10.1134/S0036023606100214.
9. *Molybdenum and Its Compounds. Applications, Electrochemical Properties and Geological Implications*, Saji, V.S. and Lopatin, S.I., Eds., New York: NOVA Publishers, 2014, ch. 16, p. 291.
10. Lopatin, S.I., *Russ. J. Gen. Chem*., 2007, vol. 77, no. 11, p. 1823. DOI: 10.1134/S1070363207110011.
11. Gunina, A.O., Lopatin, S.I., and Shugurov, S.M., *Inorg. Chem*., 2012, vol. 51, no. 9, p. 4918. DOI: 10.1021/ic201644f.
12. Berkowitz, J., Chupka, W.A., and Inghram, M.G., *J. Chem. Phys*., 1957, vol. 27, no. 1, p. 87.
13. *Energii razryva khimicheskikh svyazei. Potentsialy ionizatsii i srodstvo k elektronu* (Energy of Rapture of Chemical Bonds. Ionization Potentials and Electron Affinity), Kondrat'ev, V.N., Ed., Moscow: Nauka, 1974.
14. Mazzone, A. M. and Morandi, V., *Eur. Phys. J. (B)*, 2006, vol. 51, no. 3, p. 307. DOI: 10.1140/epjb/e2006-00227-5.
15. Zhai, H.J., Dobler, J., Sauer, J., and Wang, L.S., *J. Am. Chem. Soc*., 2007, vol. 129, no. 43, p. 13270. DOI: 10.1021/ja0750874.
16. Paule, R.C. and Mandel, J., *Pure Appl. Chem*., 1972, vol. 31, no. 3, p. 371.
17. *Recent Development in Mass Spectrometry*, Ogata, K. and Hayakawa T., Eds., Baltimore: University Park Press, 1970, p. 814.
18. Guido, M. and Gigli, G., *High Temp. Sci*., 1975, vol. 7, no. 2, p. 122.
19. *Termodinamicheskie svoistva individual'nykh veshchestv: spravochnik* (Thermodynamic Properties of Pure Substances: Handbook), Glushko, V.P., Ed., Moscow: Akad, Nauk SSSR, 1978-1984, vols. 1-4.
20. Lopatin, S.I., Semenov, G.A., and Shugurov, S.M., *Russ. J. Gen. Chem*., 2001, vol. 71, no. 1, p. 61. DOI: 10.1023/A:1012329406263.
21. Lopatin, S.I., Semenov, G.A., Baranovskii, V.I., and Sizov,, V.V., *Russ. J. Gen. Chem*., 2001, vol. 71, no. 9, p. 1342. DOI: 10.1023/A:1013985415142.
22. Baranovskii, V.I., Lopatin, S.I., and Sizov, V.V., *Russ. J. Gen. Chem*., 2000, vol. 70, no. 11, p. 1662.
23. Gusarov, A.V., *Teplofizika Vys. Temperatur*, 1970, vol. 8, no. 6, p. 1186.
24. Shugurov, S.M. and Lopatin, S.I., *Russ. J. Gen. Chem*., 2008, vol. 78, no. 5, p. 854. DOI: 10.1134/S1070363208050022.
25. Zhao, Y. and Truhlar, D.G., *Theor. Chem. Account*, 2008, vol. 120, nos. 1–3, p. 215. DOI: 10.1007/s00214-007-0310-x.
26. Linderberg, J. and Ohrn Y., *Propagators in Quantum Chemistry*, Hoboken: J. Wiley, 2004.
27. Paule, R.C. and Mandel, J., *Pure Appl. Chem*., 1972, vol. 31, no. 3, p. 397.
28. Bross, D.H., Hill, J.G., Werner, H.-J., and Peterson, K.A., *J. Chem. Phys*., 2013, vol. 139, no. 9, p. 094302. DOI: 10.1063/1.4818725.
29. Manby, F.R., *J. Chem. Phys*., 2003, vol. 119, no. 9, p. 4607. DOI: 10.1063/1.1594713.
30. May, A.J. and Manby, F.R., *J. Chem. Phys*. 2004, vol. 121, no. 10, p. 4479. DOI: 10.1063/1.1780891.

31. Werner, H.-J. and Manby, F.R., *J. Chem. Phys*., 2006, vol. 124, no. 5, p. 054114. DOI: 10.1063/1.2150817.
32. Manby, F.R., Werner, H.-J., Adler, T.B., and May, A.J., *J. Chem. Phys*., 2006, vol. 124, no. 9, p. 094103. DOI: 10.1063/1.2173247.
33. Werner, H.-J., *J. Chem. Phys*., 2008, vol. 129, no. 10, p. 101103. DOI: 10.1063/1.2982419.
34. *MOLPRO, version 2010.1*, a package of *ab initio* programs.
35. Werner, H.-J., Adler, T.B., and Manby, F.R., *J. Chem. Phys*., 2007, vol. 126, no. 16, p. 164102. DOI: 10.1063/1.2712434.
36. Kniza, G., Adler, N.B., and Werner, H.-J., *J. Chem. Phys*., 2009, vol. 130, no. 5, p. 054104. DOI: 10.1063/1.3070236.
37. Frisch, M.J., Trucks, G.W., Schlegel, H.B., Scuseria, G.E., Robb, M.A., Cheeseman, J.R., Scalmani, G., Barone, V., Mennucci, B., Petersson, G.A., Nakatsuji, H., Caricato, M., Li, X., Hratchian, H.P., Izmaylov, A.F., Bloino, J., Zheng, G., Sonnenberg, J.L., Hada, M., Ehara, M., Toyota, K., Fukuda, R., Hasegawa, J., Ishida, M., Nakajima, T., Honda, Y., Kitao, O., Nakai, H., Vreven, T., Montgomery, J.A., Jr., Peralta, J.E., Ogliaro, F., Bearpark, M., Heyd, J.J., Brothers, E., Kudin, K.N., Staraboveov, V.N., Keith, T., Kobayashi, R., Normand, J., Raghavachari, K., Rendell, A., Burant, J.C., Iyengar, S.S., Tomasi, J., Cossi, M., Rega, N., Millam, J.M., Klene, M., Knox, J.E., Cross, J.B., Bakken, V., Adamo, C., Jaramillo, J., Gomperts, R., Stratmann, R.E., Yazyev, O., Austin, A.J., Cammi, R., Pomelli, C., Ochterski, J.W., Martin, R.L., Morokuma, K., Zakrzewski, V.G., Voth, G.A., Cioslowski, J., and Fox, D.J., *GAUSSIAN 09,* Revision D.01. Gaussian, Inc., Wallingford CT. 2010.
38. Weigend, F. and Ahlrichs, R., *Phys. Chem. Chem. Phys.*, 2005, vol. 7, no. 18, p. 3297. DOI: 10.1039/b508541a.
39. *http: // www.chemcraftprog.com.*
40. Hanwell, M.D., Curtis, D.E., Lonie, D.C., Vandermeersch, T., Zurek, E., and Hutchison, G.R., *J. Cheminform*., 2012, vol. 4, no. 8, p. 17. DOI: 10.1186/1758-2946-4-17.
41. Lopatin, S.I. and Shugurov, S.M., *Open Thermodyn. J.,* 2013, vol. 7, suppl. 1, p. 35. DOI: 10.2174/1874396X01307010035.
42. Kunkel, K., Milke, E., and Binnewies, M., *Int. J. Mass Spectrom*., 2014, vol. 374, p. 12. DOI: 10.1016/j.ijms.2014.09.019.
43. Shugurov, S.M. and Lopatin, S.I., *Russ. J. Gen. Chem*., 2008, vol. 78, no. 10, p. 1882. DOI: 10.1134/S1070363208100095.
44. Shugurov, S.M., Lopatin, S.I., and Gunina, A.O., *Russ. J. Gen. Chem*. 2008, vol. 77, no. 9, p. 1487. DOI: 10.1134/S1070363207090022.
45. Shol'ts, V.B. and Sidorov, L.N., *Vestn. MGU, Ser. Khim*., 1972, vol. 13, no. 4, p. 371.